Hydration of the sulfate dianion in cold nanodroplets: SO 4 2– (H 2 O) 12 and SO 4 2– (H 2 O) 13

Florian Thaunay, Carine Clavaguéra, Gilles Ohanessian

PCCP

PAPER

Cite this: *Phys. Chem. Chem. Phys.*, 2015, **17**, 25935

Hydration of the sulfate dianion in cold nanodroplets: $SO_4^{2-}(H_2O)_{12}$ and $SO_4^{2-}(H_2O)_{13}$†

Florian Thaunay, Carine Clavaguéra and Gilles Ohanessian*

Received 1st May 2015,
Accepted 15th June 2015

DOI: 10.1039/c5cp02557e

www.rsc.org/pccp

The structures, energetics and infrared spectra of $SO_4^{2-}(H_2O)_{12}$ and $SO_4^{2-}(H_2O)_{13}$ have been investigated by a combination of classical polarizable molecular dynamics and static quantum chemical calculations. Snapshots extracted from MD trajectories were used as inputs for local DFT optimization. Energies of the most stable structures were further refined at the *ab initio* level. A number of new low energy structures have thus been identified. The most stable structures of $SO_4^{2-}(H_2O)_{12}$ have the sulfate on the surface of the water cluster, while it may be slightly more burried in $SO_4^{2-}(H_2O)_{13}$, however still with an incomplete first hydration shell. Differences in the infrared spectra arise in part from mixing of sulfate stretching and water librational modes in the 900–1100 cm^{-1} region, leading to some sensitivity of the IR spectrum to the structure. Second shell water molecules however do not generate signatures that are specific enough to relate spectra to structures straightforwardly, at least in this frequency range. Thus the emergence of a new band at 970 cm^{-1} in the $SO_4^{2-}(H_2O)_{13}$ spectrum cannot be taken as a clue as to the number of water molecules which is necessary for a cluster to close the first hydration shell of sulfate. This number is at least 14 and possibly larger. However the density of low energy isomers is large enough that individual structures may loose meaning at all but the lowest temperatures.

1. Introduction

Hydrates of the sulfate dianion SO_4^{2-} are found to be key components in the environment as well as in several biological contexts. They are present in the atmosphere as aerosol particles.[1,2] Field measurements show that nucleation rates correlate with the concentration of sulfuric acid, eventually leading to the formation of cloud condensation nuclei.[3] Aerosols of hydrated sulfate also play a key role in the homogeneous nucleation of ice particles in the upper troposphere.[4] In biological context, SO_4^{2-} is an important cell nutriment and the fourth most abundant anion in mammalian plasma. However as a hydrophilic anion, it requires a transporter inward and outward of cells. Such a mechanism is regulated by the competition between ion hydration and capture by a macromolecule.[5] Thus a detailed understanding of sulfate hydration and its competition with other media is of high importance in a number of contexts.

A first step towards this understanding is the knowledge of the structure and dynamics of bare sulfate in water. To this end, sulfate–water cluster $SO_4^{2-}(H_2O)_n$ in the gas phase are appropriate prototype systems. Thus it is not surprising that these clusters have been the subject of intense research for more than a decade. While most early studies focused on small clusters in the n = 3–6 range, data have now grown to encompass n ranging from 3 to 80[6] and even *ca.* 250.[7]

The gaseous sulfate dianion is unstable against electron detachment.[8–10] It has been shown that stabilizing the dianion requires three water molecules, *i.e.* $SO_4^{2-}(H_2O)_3$ is the smallest stable sulfate hydrate in the gas phase.[10,11] Small clusters in the n = 3–7 range have been extensively characterized.[12–21] In particular computational investigations by Head-Gordon *et al.* have provided both a comprehensive picture of the low energy structure manifold[19] and a thorough calibration of the performances of quantum chemical methods.[20] Many density functionals were compared to *ab initio* results at the current accuracy limit.[21]

There have been several reports of quantum chemical computations for n = 12.[13,14,23,24,27] They were largely limited to the same shell-closing 12+0 structure (named W12-AN below) although Wong and Williams[24] found that many structures with varying numbers of molecules in the second shell are expected to lie in a small energy window, and Gao and Liu[14] did report a 9+3 structure (named W12-GL below) which they found to be significantly more stable than 12+0. A recent work reported by Galli *et al.*[27] appears to be the first to address the issue of whether or not the first hydration shell of sulfate is closed at n = 12. In a Born–Oppenheimer molecular dynamics (MD) study carried out using the PBE and PBE0 functionals, these authors found structures with the sulfate on the cluster surface which were slightly more stable than those invoked previously, with the sulfate in the

Laboratoire de chimie moléculaire, Ecole polytechnique, CNRS, 91128 Palaiseau Cedex, France. E-mail: gilles.ohanessian@polytechnique.edu

† Electronic supplementary information (ESI) available. See DOI: 10.1039/c5cp02557e

interior of the water cluster. Comparison between computed and experimental IR spectra showed that both types of structures are compatible with experiment (both infrared (IR) and photoelectron spectra). The authors concluded that both may be formed as a mixture under the experimental conditions used.

A number of experimental techniques have been used to characterize the properties of $SO_4^{2-}(H_2O)_n$ in a wide size range. Photoelectron spectra at room temperature of n = 3–40[22] displayed several bands corresponding to rather different binding energies, and gradual changes with increasing size. In particular, the relative intensity of the low binding energy feature arising from SO_4^{2-} decreases and almost disappears in the large clusters, while a very intense peak emerges at the high binding energy side. This was interpreted as indicating that electron detachment occurs from the sulfate in the small size regime, while it occurs from the water cluster for larger sizes. While this strongly suggests that the sulfate ion is deeply buried inside the water droplet for the larger clusters, there appeared to be no breaking point which would provide a clear indication of a structural transition in a specific size range.

IR spectra were recorded at low temperature in the n = 3–24 range.[23] Direct comparison with the spectrum in bulk water suggested easy band assignments to either sulfate or water bands. Splittings observed for specific sizes between the sulfate antisymmetric stretching bands were used to infer structure information. In addition, the appearance of a new band in the n = 13 spectrum was taken as an indication that the first hydration shell may be complete at n = 12, with the 13th molecule bound in a different manner, most probably in the second shell. Earlier BIRD experiments,[24] whereby the rate of water evaporation can be determined for each cluster size, did indicate a break at n = 12, with a similar interpretation. Finally, high pressure mass spectrometric experiments[25,26] yielded size-selective binding enthalpies and entropies. These results showed a relatively uniform trend with size, with no specific properties for n = 12. However the authors noted that the populations of structures undergoing dissociation may be different if BIRD experiments involve non-Boltzmann distributions. The temperature dependence of isomer populations has also been pointed out for smaller clusters in the discussion of photoelectron spectra.[18] Thus the question of the existence of a structural transition between n = 12 and 13 remains partly unsettled from the experimental point of view.

In the present paper we reconsider the structures of $SO_4^{2-}(H_2O)_{12}$ and $SO_4^{2-}(H_2O)_{13}$ from a computational viewpoint and attempt to provide answers to the following questions: (i) is there a shell-closing transition for these clusters, and (ii) how structure-telling are IR spectra in the fingerprint region in this size range?

2. Computational details

The potential energy surfaces for n = 12 and 13 were explored using a combination of molecular dynamics (MD) using a classical force field and of quantum chemical calculations. MD simulations were carried out using the polarizable AMOEBA force field (using the AMOEBA03 parameters for water as available in the Tinker software[31] and the sulfate parameters from ref. 19). They were propagated from several starting points chosen to ensure both structural and energetic diversity. Snapshots extracted from these trajectories at regular intervals were then used as starting points for local geometry optimization using density functional theory (DFT), followed by vibrational spectrum calculations in the harmonic approximation. Final energetics were refined at the *ab initio* level. The details of these procedures are detailed below.

Simulations for n = 12 started from 3 structures: the most often invoked in the literature[13,14,23,24,27] has all water molecules, arranged in four $(H_2O)_3$ clusters, interacting with the sulfate oxygens thereby forming a closed first hydration shell. With no H_2O in the second shell, this structure is thus described as 12+0. A second structure from the literature,[14] described as more stable than the previous, in which three $(H_2O)_4$ clusters surround the sulfate ion. Each has one H_2O in the second shell, making this a 9+3 type structure. (iii) Another 12+0 structure manually generated to be less symmetrical than the previous, in which the sulfate ion is closer to the cluster surface, although the total numbers of sulfate–water (12) and water–water (12) hydrogen bonds are the same. From each of these 3 structures, MD trajectories were propagated using the Beeman integrator, and a time step of 1 fs. The temperature was first raised from 0 to 200 K in the *NVT* ensemble for 2 ps, using the Nosé-Hoover thermostat. The trajectory was then propagated for 3 ns at 200 K in the *NVE* ensemble. Snapshots were extracted at 100 ps time intervals. This time step is much larger than that for any relevant vibrational mode. We expect that exchange between conformations may require a number of vibration periods, thus selecting snapshots with a much smaller time interval may generate a large fraction of redundancies. In order to scan the energy surface extensively, a large time interval may be more efficient. On the other hand, the value taken here is probably too large to ensure a thorough identification of all low energy structures. Rather, our aim here is to identify all low energy *structural families*. Snapshots at 200 ps intervals were then subjected to geometry optimization using the M11 density functional and the 6-311++G(d,p) atomic basis set; M11 has been shown to be accurate on relative energies for n = 3–7 by Head-Gordon *et al.*[21] Whenever two consecutive optimized structures were within 10 kJ mol^{-1} of the lowest in energy so far, an additional calculation was run using the intermediate snapshot from MD, thus reducing the time interval from 200 to 100 ps. A total of 71 DFT calculations were run in this manner.

Simulations for n = 13 followed essentially the same lines as for n = 12. Starting structures were manually constructed by adding one H_2O to previously obtained structures of $SO_4^{2-}(H_2O)_{12}$ from four different families: three structures were used as starting points for n = 12 and the most stable 9+3 type structure found at the *ab initio* level. This ensures structural diversity as well as some very low energy starting points. The exact same procedure was used throughout as described above for n = 12, except for using 4 starting structures instead of 3 and propagating each trajectory for 4 instead of 3 ns. This generated a total of 99 DFT calculations.

Some considerations of the efficiency of the exploration procedure are provided in the ESI,† see Section S-1.

As described previously for clusters with n = 3–7,[19] the energy ordering is modified by inclusion of zero-point vibrational energy (ZPE). Thus all results below include ZPE computed at the M11 level. These are however not corrected for entropy effects since experiments in ref. 23 were carried out at 17 K, where they are negligible. Computations indicate that entropy effects would be significant at room temperature.

Vibrational spectra were computed at the M11/6-311++G(d,p) level. Sulfate frequencies, especially those of the antisymmetric group of bands of central interest in this work, turned out not to require scaling. This has been observed before with other density functionals[28] and also for the phosphate vibrational frequencies.[29] It would be conceivable to use a standard scaling for water bands and none for sulfate bands, however the 900–1100 cm^{-1} region was found to involve significant mixing between some water libration and sulfate stretching motions. Therefore it appeared more appropriate to use no scaling for any band.

Considering the rather complex manifolds of low energy structures, it was deemed important to obtain final energetics at more accurate levels than M11/6-311++G(d,p). To this end, energetics at the M11 geometries were obtained at a number of levels, including M11/aug-cc-pVTZ, MP2, CC2 and the recently developed Domain-based Local Pair Natural Orbital approximation to CCSD(T) [DLPNO-CCSD(T)][30] levels. Each of these post-Hartree–Fock levels was combined with both the TZVPP and aug-cc-pVTZ basis sets. All the results are gathered in Tables S1 for n = 12 and S2 for n = 13 (ESI†). Only those obtained at the highest level, DLPNO-CCSD(T)/aug-cc-pVTZ//M11/6-311++G(d,p), are reported in Tables 1 and 2 and in the text below.

MD calculations were run using the Tinker 6 package.[31] DFT calculations were done using the Gaussian09 package.[32] MP2 and CC2 wavefunctions were computed using the Turbomole 6.6 package.[33] DLPNO-CCSD(T) wavefunctions were computed using the Orca 3.0.3 package.[34]

Table 1 Relative energies (kJ mol^{-1}) of low energy structures of $SO_4^{2-}(H_2O)_{12}$, computed at the DLPNO-CCSD(T)/aug-cc-pVTZ//M11/6-311++G(d,p) level with M11-computed 0 K vibrational energies. Structures with names in bold are displayed in Fig. 1, with IR spectra in Fig. 2

Structure name	Coordination of sulfate oxygens	Relative energy
W12-1a	[3,2,2,2]	0.0
W12-1b	[3,2,2,2]	0.0
W12-1c	[3,2,2,2]	2.1
W12-1d	[3,2,2,2]	6.2
W12-2	[3,3,3,3]	8.2
W12-3	[3,"3","3",2]	8.5
W12-4	[3,2,2,2]	8.9
W12-5	[3,"3","3",2]	10.0
W12-6	[3,3,2,2]	10.2
W12-7	[3,2,2,2]	10.8
W12-8	[3,"3","3",2]	12.9
W12-9	[3,"3","3",2]	13.1
W12-10	[3,2,2,2]	13.3
W12-11	[3,3,3,2]	17.7
W12-GL	[4,2,2,2]	19.0
W12-AN	[3,3,3,3]	27.0

3. Results

A. Structures and energetics of $SO_4^{2-}(H_2O)_{12}$

A total of 71 structure optimizations were carried out at the DFT level for $SO_4^{2-}(H_2O)_{12}$. The low-energy results are summarized in Fig. 1 and 2 and in Table 1. A recurring motif, well known in pure water clusters, is the cyclic tetramer. It bears one dangling OH bond per water molecule, in alternating orientations relative to the oxygen network in the most stable structure of $(H_2O)_4$. Only slightly higher in energy lies the cyclic tetramer with all dangling OH bonds pointing in roughly the same direction. Among the most stable hydrated sulfate clusters studied herein, this $(H_2O)_4$ structure is found as a common building block, as it is well adapted to binding to three sulfate oxygens, while the fourth dangling OH can be oriented towards an oxygen of another water cluster (*e.g.* another tetramer). This fourth OH belongs to a water molecule lying in the second hydration shell of the sulfate ion, while the other three are in the first shell. The cluster can also receive a hydrogen bond from a third water cluster on its other side. Putting side to side three such clusters makes the most stable structure of $SO_4^{2-}(H_2O)_{12}$, W12-1a as shown in Fig. 1. It is of 9+3 type, indicating that 9 water molecules are in the first and 3 are in the second hydration shell. In addition, each tetramer can accommodate degenerate reversal of its cyclic hydrogen bonding orientation. Interactions with sulfate and with other water clusters make this reversal no longer degenerate in the present case; however energy differences were found to be only a few kJ mol^{-1}, see W12-1b to W12-d. Since hydrogen bonding orientation reversal can occur in a single tetramer or in two or three simultaneously, seven very similar structures can thus be generated for this particular motif.

With a heavy atom skeleton of C_3 symmetry, three of the sulfate oxygens in the most stable structures W12-1a to W12-1d are 2-coordinated and lie at the cluster surface while the fourth oxygen is 3-coordinated in the cluster interior. Thus the coordination shell scheme is 9+3 and the sulfate oxygen coordination pattern is [3,2,2,2]. W12-b to W12-d are all deduced from W12-a by reversal of some of the hydrogen bonds. Two views of W12-1b are shown in Scheme 1; the left view highlights the position of the sulfate ion near the water cluster surface. The right view is a top view along an S–O axis with the interior O in the back. The latter perspective is chosen for all other W12-1 isomers shown in Fig. 1 to highlight the hydrogen bond network.

The first structure with a complete hydration shell around the ion is W12-2. It is made of 3 water trimers, each making a 4-membered ring with one of the sulfate oxygens. This motif is quite stable, probably one of the low energy structures of $SO_4^{2-}(H_2O)_9$. W12-2 is completed with a cyclic water trimer donating 3 hydrogen bonds to 3 sulfate oxygens (shown at the top of W12-2 in Fig. 1). This structure is less stable than W12-1 by 8.2 kJ mol^{-1}. It is quite different from, and much more stable than, the shell-completing isomer W12-AN invoked previously as the most stable of $SO_4^{2-}(H_2O)_{12}$: the latter is computed to lie 27.0 kJ mol^{-1} higher in energy than W12-1 and 18.8 kJ mol^{-1} higher than W12-2. Another isomer, W12-3, although it is quite different than W12-2, has a nearly complete hydration shell,

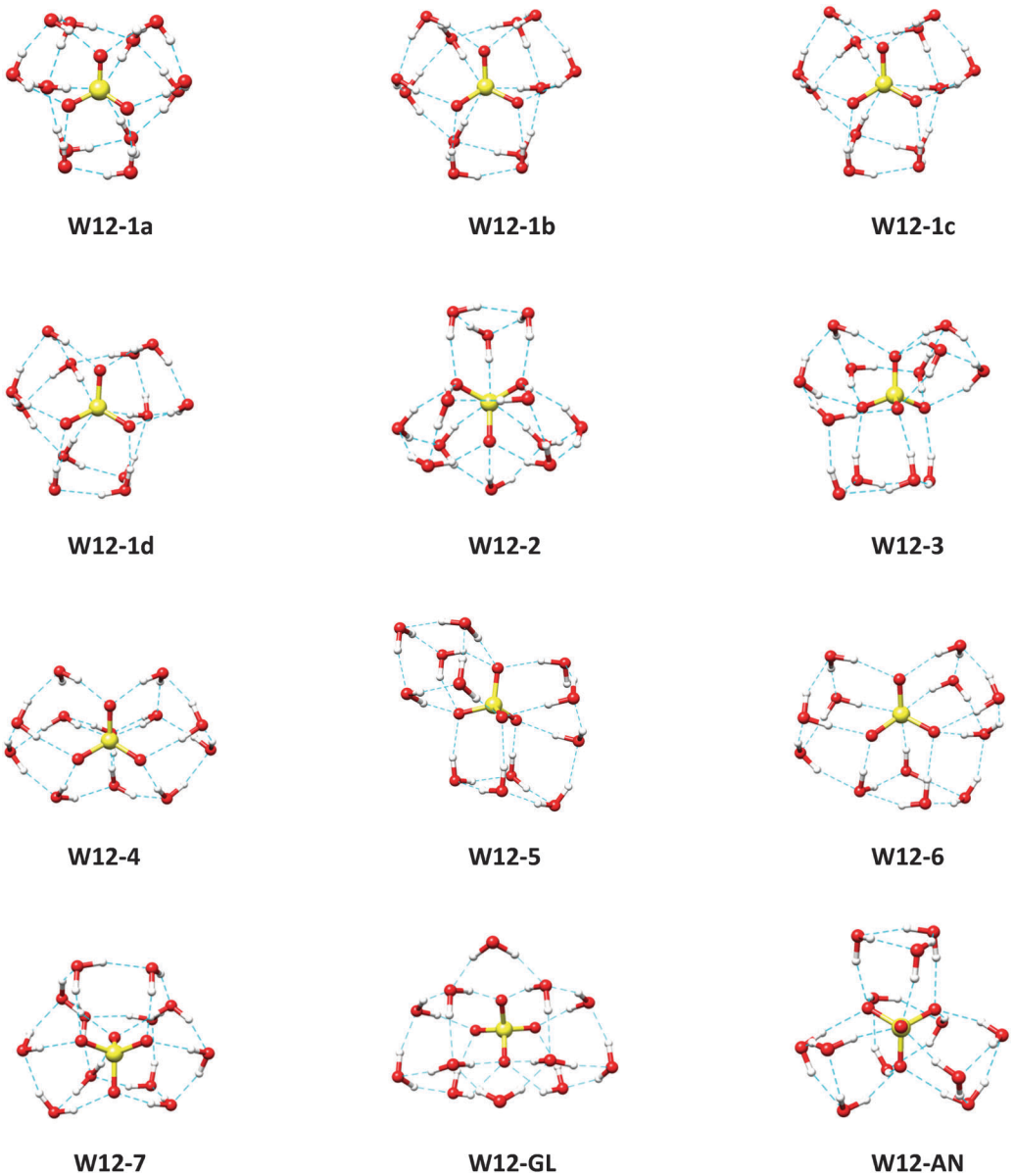

Fig. 1 Structures of low energy isomers of $SO_4^{2-}(H_2O)_{12}$. The ordering in "W12-*x*" is based on DLPNO-CCSD(T)/aug-cc-pVTZ//M11/6-311++G(d,p) relative energies, including M11 zero-point vibrational energies. "W12-AN" is from ref. 23.

although a single water molecule bridges between two sulfate oxygens with larger hydrogen bonding distances.

The next most stable structure W12-4 is distorted from W12-1 with only two water tetramers connected in a fused manner by a $(H_2O)_5$ cluster. It is also of 9+3 and [3,2,2,2] types. W12-5 has two distorted "cube-like" structures involving five H_2O and the sulfate. The next structures in the energy list (W12-6 and W12-7) have rather similar global shapes, somewhat "2-dimensional" with the sulfate again near the cluster surface. Finally, the 9+3 isomer W12-GL, the most stable found in a previous study,[14] is also included for comparison. It is confirmed to be significantly more stable than W12-AN, however the large difference with W12-1 makes it very unlikely to be observable experimentally. The present search thus leads to a complete reappraisal of the structures and energies of $SO_4^{2-}(H_2O)_{12}$, since most of the above structures had not been identified before. The notable exception is the work by Galli *et al.*[27] who did find surface-bound sulfate among the low energy structures.

Scheme 1

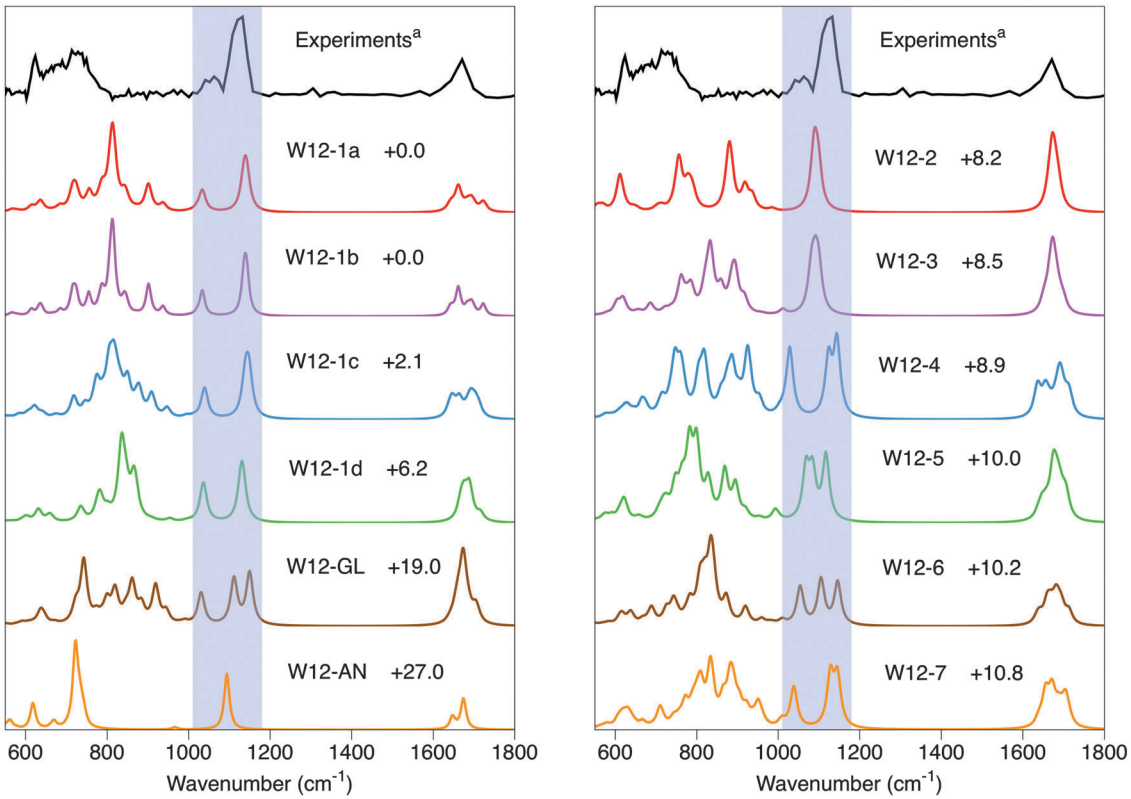

Fig. 2 Experimental IRPD spectrum (ref. 23, top) and computed absorption spectra of several low energy isomers of $SO_4^{2-}(H_2O)_{12}$. Structures and spectra are at the M11/6-311++G(d,p) level. Relative energies, in kJ mol^{-1}, are at the DLPNO-CCSD(T)/aug-cc-pVTZ level using the same geometries.

In the most stable structures W12-1a to W12-1d, the water–water hydrogen bond lengths range from 1.86 to 1.95 Å, the shortest are made by water molecules interacting with the sulfate; globally expanded relative to those in the equivalent free water tetramer (1.83 and 1.91 Å in a puckered conformation). The inter-cluster bonds are all near 1.91 Å. The water–sulfate hydrogen bonds are all very similar, ranging from 1.86–1.90 Å. While these values are typical of many other structures, there is some variation associated with the types of water clusters formed around the ion: in the 3-membered rings of W12-AN, they are significantly longer at 1.98 Å because of larger cyclic strain, while the water–sulfate distances of 1.92 Å are only slightly longer than for 4-membered rings.

Very recently, a sophisticated basin-hopping Monte Carlo algorithm for potential energy surface exploration was used to survey the low energy structures of $SO_4^{2-}(H_2O)_n$, n = 3–50.[35] A rigid-body potential was used to calculate energies, TIP4P for water and fixed atomic charge electrostatic plus 12-6 Lennard-Jones interaction terms for the sulfate ion.[36] The low energy structures identified are W12-AN and (similar to) W13-AN for $SO_4^{2-}(H_2O)_{12}$ and $SO_4^{2-}(H_2O)_{13}$, respectively. As described above, these are high energy structures, at least 20 kJ mol^{-1} above the lowest energy structure found herein. This large energy discrepancy is reflected by rather different mean hydrogen bond lengths computed with the force field and with M11/6-311++G(d,p), for the 12+0 structure of $SO_4^{2-}(H_2O)_{12}$: ~1.87 *vs.* 1.98 Å for water–water and ~1.79 *vs.* 1.92 Å for sulfate–water hydrogen bonds, respectively. This force field favors 3-membered water rings interacting with 2 sulfate O's, while we find that 4-membered rings are distinctly more stable, at least in this size range. Thus the use of a rigid-body, non-polarizable potential with simple electrostatics to calculate energies does not appear to provide enough accuracy to identify low energy structures reliably.

B. IR spectra of $SO_4^{2-}(H_2O)_{12}$

As discussed in ref. 23, the IR spectra of $SO_4^{2-}(H_2O)_n$ are expected to be easy to interpret, based on the known IR spectrum of sulfate in bulk water. The sulfate bending and antisymmetric stretching bands are expected to arise near 600 and 1100 cm^{-1}, respectively, while water libration and bends should appear as wide features centered at around 800 and 1600 cm^{-1}, respectively. This is what is observed in most experimental spectra for n = 3–14, 18 and 24,[23] with water bands rising in width and intensity relative to those of sulfate, for clusters of growing size. Some of the details in band shapes were used as structural fingerprints, especially for structures involving different levels of symmetry breaking in small clusters. As shown below, this simple scenario does not appear to hold in the 900–1100 cm^{-1} range with extensive water–sulfate mixing in some of the normal modes for n = 12 and n = 13.

Computed spectra are displayed in Fig. 2. The lowest energy structures W12-1a-d have rather similar spectra as expected, except in the water libration massif for W12-1c and W12-1d. Band assignments will therefore be detailed for W12-1a only.

Three intense bands appear in the 1000–1200 cm^{-1} range. The most intense at 1136 and 1143 cm^{-1} correspond to sulfate stretching motions involving primarily the three S–O bonds on the cluster surface. The band at 1034 cm^{-1} is a combination dominated by the libration of several water molecules, with a minor contribution of sulfate stretching arising mainly from the S–O bond pointing towards the water cluster. These three bands account well for the experimental doublet in the 1000–1200 cm^{-1} area with the component to the blue being much more intense. A second combination with the ''inside'' sulfate stretching as the major component and water libration as the minor component is found at 938 cm^{-1}, to the blue of two more intense, delocalized water libration bands at 901 and 902 cm^{-1}. There are several weak bands in the 600–620 cm^{-1} range with significant components of sulfate bending modes, in addition to water. All of the features above, plus the water bending feature in the 1630–1710 cm^{-1} region, agree rather well with the experimental bands. It is less true for the large feature from 600 to 800 cm^{-1}, for which the computed frequencies appear to be systematically overestimated.

The computed spectra of W12-4 and W12-7 are similar to those of the W12-1 series in the 1000–1200 cm^{-1} range, while the higher IR activity in 900–1000 cm^{-1} range appears to be in less good agreement with experiment. The spectra of W12-2, W12-3 and W12-AN all have a single feature between 1000 and 1200 cm^{-1}, in disagreement with experiment. These 3 structures have complete or nearly complete hydration shells forming identical or similar bonding environments for all sulfate oxygens, leading to three very similar sulfate stretching frequencies. This highlights the inconsistency of the n = 12 spectrum with a saturated first shell. The reverse situation occurs for W12-6 in which although the sulfate is on the cluster surface, it has an unsymmetrical coordination motif with one of the surface oxygen bound to three H_2O. This lifts band degeneracy to yield three well separated bands at 1054, 1105 and 1146 cm^{-1}, clearly at variance with the experimental spectrum. For all of these structures the sulfate and water bending frequencies are rather insensitive to structural details, while the water libration group of bands is much more sensitive, however always to the blue of the experimental feature except in the case of W12-AN for which it is well positioned, albeit much too narrow because of the high symmetry.

The results described above do not fit with the shell-closing picture at n = 12, both from computed energetics and from comparison of computed and experimental IR spectra. Three S–O bonds of the sulfate are found to lie at the cluster surface in the several most stable structures, with the first 12+0 isomer lying 8.2 kJ mol^{-1} higher in energy than the most stable one. The computed IR spectra also challenge the view that band assignments can be safely made on the basis of those established for the bulk spectrum in the 900–1200 cm^{-1} region.

C. Structures and energetics of $SO_4^{2-}(H_2O)_{13}$

A total of 99 structure optimizations were carried out at the DFT level for $SO_4^{2-}(H_2O)_{13}$. The low-energy results are summarized in Fig. 3 and 4 and in Table 2. All structures lying in an energy window of 10 kJ mol^{-1} are listed in Table 2, and a selection is shown in Fig. 3 and 4.

Table 2 Relative energies (kJ mol^{-1}) of low energy structures of $SO_4^{2-}(H_2O)_{13}$, computed at the DLPNO-CCSD(T)/aug-cc-pVTZ//M11/6-311++G(d,p) level with M11-computed 0 K vibrational energies. Structures with names in bold are displayed in Fig. 3, with IR spectra in Fig. 4

Structure name	Coordination of sulfate oxygens	Relative energy
W13-1a	[3,2,2,2]	0.0
W13-2	[3,2,2,2]	1.2
W13-3	[3,2,2,2]	2.9
W13-4	[3,2,2,2]	3.1
W13-1b	[3,2,2,2]	3.1
W13-1c	[3,2,2,2]	3.1
W13-5	[3,3,3,2]	3.2
W13-1b2	[3,2,2,2]	3.5
W13-6	[3,3,2,2]	3.6
W13-2b	[3,2,2,2]	4.0
W13-1b3	[3,2,2,2]	4.3
W13-1b4	[3,2,2,2]	4.4
W13-1d	[3,2,2,2]	5.1
W13-7	[3,''3'',''3'',2]	5.3
W13-8	[3,2,2,2]	5.7
W13-9	[3,3,3,''3'']	6.1
W13-1d2	[3,2,2,2]	6.3
W13-10	[3,3,3,''3'']	6.3
W13-1e	[3,3,2,2]	6.5
W13-11	[3,2,2,2]	8.3
W13-12	[3,3,2,2]	9.9
W13-13	[3,3,2,2]	9.9
W13-AN	[3,3,3,3]	19.5

As for $SO_4^{2-}(H_2O)_{12}$, a number of isomers of $SO_4^{2-}(H_2O)_{13}$ were found to be similar in the sense that their oxygen network and connectivity are identical and they differ only by the partial reversal of the hydrogen bonds. Another type of similarity is when the 13th water molecule is added to one of the several sites of a single $SO_4^{2-}(H_2O)_{12}$ core. A particularly clear case is that of W12-1. To this structure, the 13th water molecule can be added either to a ''vertical'' or a ''horizontal'' edge of one of the $(H_2O)_4$ clusters (in the orientation shown in Fig. 3, see W13-1d and W13-1c), or bridging between two such clusters (W13-1a), or bridging between one cluster and a sulfate oxygen (W13-1e), or bridging between two sulfate oxygens (W13-1b). This W13-1 structural family is found to span an energy range of at least 6.5 kJ mol^{-1} (see Table 2).

While W13-1a is the most stable structure found for n = 13, there are several other structure types which appear in the lower energy manifold. They are based on the same building blocks described above for n = 12. Cubic-like fragments can be seen in most structures among W13-2 to W13-7. Additional water cluster fragments are also found, including a cyclic pentamer. As for the tetramer described above, the pentamer can donate OH's to three sulfate oxygens, however its larger size allows it to donate two and receive one hydrogen bonds with other water clusters. The most stable structures with nearly complete first hydrations shells are W13-9 and W13-10 (not shown in Fig. 3 and 4), 6.1 and 6.5 kJ mol^{-1} higher in energy than W13-1a. Both have a water molecule bridging between two sulfate O's, with bond distances larger than those for a truly saturated case such as W13-AN, the structure previously invoked in ref. 23 whose

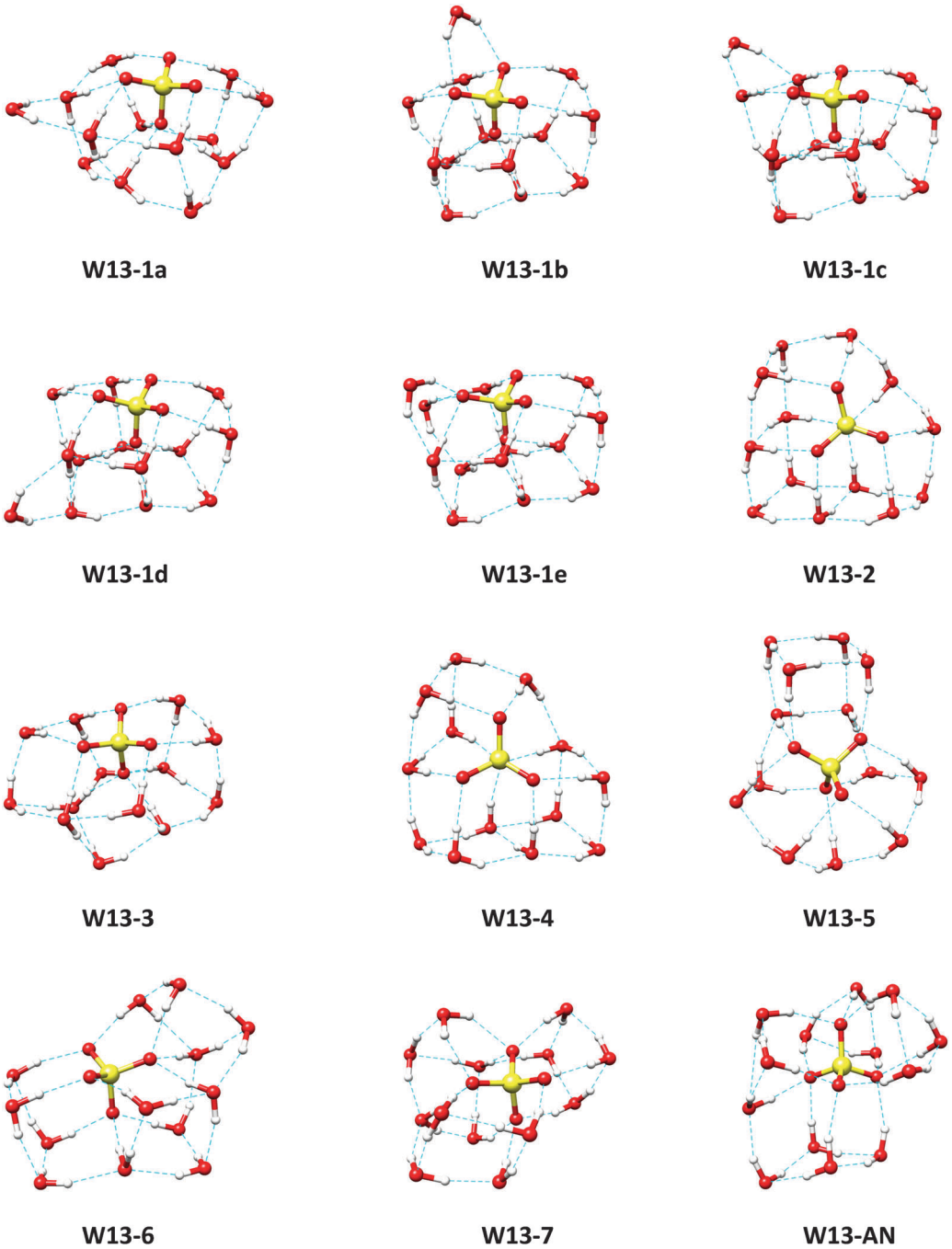

Fig. 3 Structures of low energy isomers of $SO_4^{2-}(H_2O)_{13}$. W13-AN is from ref. 23. The ordering in "W13-x" is based on DLPNO-CCSD(T)/aug-cc-pVTZ//M11/6-311++G(d,p) relative energies, including M11 zero-point vibrational energies.

energy is 19.5 kJ mol^{-1} higher than that of W13-1a. Thus this 12+1 structure cannot contribute to the IR spectrum.

Finally, comparison of Tables 1 and 2 shows that the low energy density of isomers is significantly larger for $n = 13$ than it is for $n = 12$.

D. IR spectra of $SO_4^{2-}(H_2O)_{13}$

As discussed above for $SO_4^{2-}(H_2O)_{12}$, most of the bands in the IR spectrum of $SO_4^{2-}(H_2O)_{13}$ can be readily assigned to specific sulfate or water motions, except in the 900–1100 cm^{-1} range where coupling occurs between the stretching of the inside S–O bond and some water librations.

The lowest energy structure, W13-1a, has a $(H_2O)_{12}$ core identical to W12-1. Most of their vibrational bands being very similar, only the most relevant features and the main differences will be mentioned below. For instance the pure sulfate antisymmetric stretching bands appear at 1130 and 1153 instead of 1136 and 1143 cm^{-1}, slightly more different because of the symmetry breaking effect of the 13th water molecule. Again the band at 1037 cm^{-1} is a combination

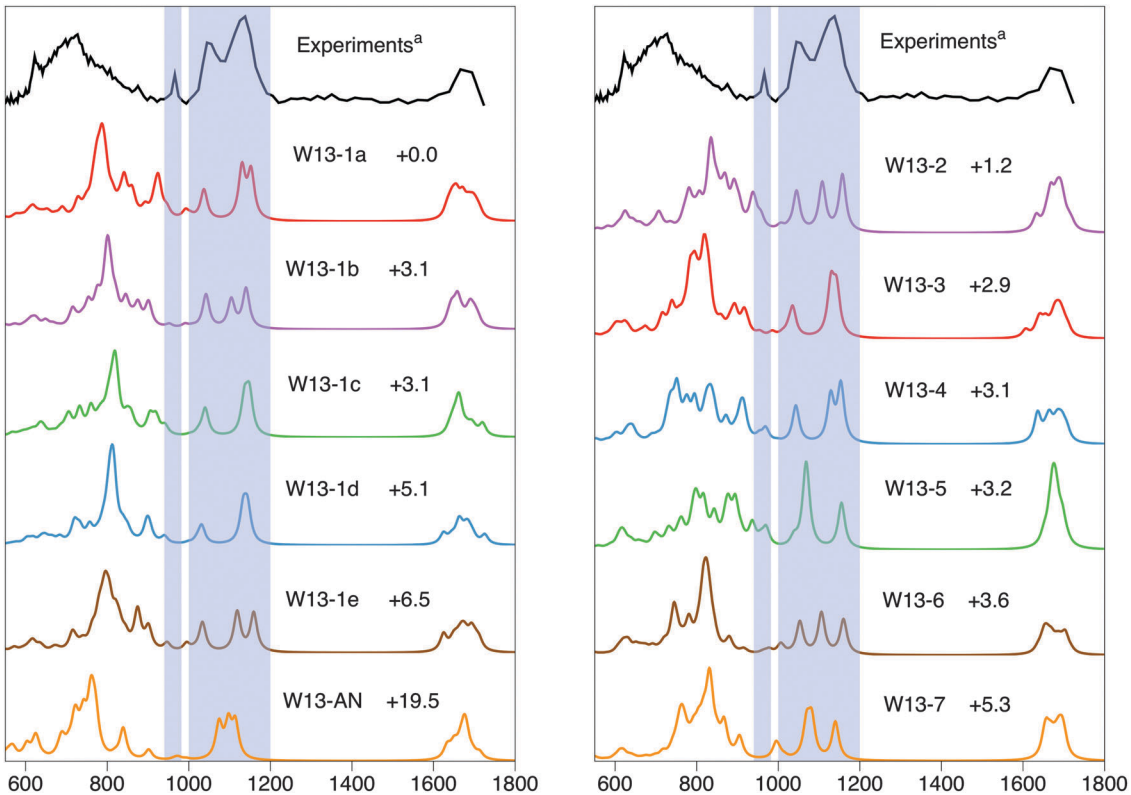

Fig. 4 Experimental IRPD spectrum (ref. 23, top) and computed absorption spectra of several low energy isomers of $SO_4^{2-}(H_2O)_{13}$. Structures and spectra are at the M11/6-311++G(d,p) level. Relative energies, in kJ mol^{-1}, are at the DLPNO-CCSD(T)/aug-cc-pVTZ level using the same geometries.

dominated by the libration of several water molecules, with a minor contribution of sulfate stretching arising mainly from the S–O bond pointing towards the water cluster. These three bands account well for the intense experimental features in the 1000–1200 cm^{-1} area. A second combination with the "inside" sulfate stretching being the major component and water libration minor is found at 946 cm^{-1}. It is our best candidate to account for the experimental band at 970 cm^{-1}. To the blue of the previous band lie two more intense water libration bands at 917 and 925 cm^{-1}, blue-shifted relative to the analogous bands in the spectrum of W12-1. None of the above libration motions involve a significant component from the "13th" water molecule. The most intense is the coupled motion of the two water molecules which are bound to the sulfate and receive hydrogen bonds for the outer water, the latter making their motion more constrained and thus blue-shifted. Finally a less intense band at 992 cm^{-1} arises from coupled librations in one of the water tetramers, to which the outer water is bound. This is a second possible assignment for the experimental band at 992 cm^{-1}. As for $SO_4^{2-}(H_2O)_{12}$, there are several weak bands in the 600–620 cm^{-1} range with significant components of sulfate bending modes. All of the features above, plus the water bending bands in the 1630–1710 cm^{-1} region, agree rather well with the experimental bands. It is less true for the large feature from 600 to 900 cm^{-1}, for which the computed frequencies appear to be systematically overestimated.

Structures W13-1b to W13-1e, in which the 13th water molecule occupies different binding sites of a common $SO_4^{2-}(H_2O)_{12}$ core which is essentially the same as W12-1, have similar computed spectra as expected. Some easily discernible differences arise from the local interactions in the various binding sites. Near degeneracy of the surface S–O bond stretch frequencies occurs for W13-1c and W13-1d in which the additional water molecule bind to an edge of a $(H_2O)_4$ cluster, either horizontal in 1c or vertical in 1d, far away from the sulfate ion. When it bridges between a sulfate and a water O, or between two of the sulfate Os, degeneracy is lifted again (W13-1e and W13-1b). In all cases a sulfate stretch motion combined to some water libration gives rise to a relatively weak band in the 940–950 cm^{-1} range.

Inspection of Fig. 4 indicates that the spectra computed for the other low energy structures, W13-2 to W13-6, are all relatively similar to those described above for W13-1b to W13-1e. Again the varying degree of degeneracy of the sulfate stretching bands can be traced to the more or less symmetrical environment of the sulfate S–O bonds, both on the surface and in the interior of the water cluster since the structures are more different. The spectra of W13-2, W13-4 and W13-5 all display a sulfate stretching band in the 940–970 cm^{-1} range.

The spectrum of W13-4 may have the best overall agreement with the experimental spectrum, especially since it displays a band at 969 cm^{-1} and a weaker one at 953 cm^{-1} (not resolved in Fig. 4). Both arise from libration of water molecules in a four-membered ring, coupled to stretching of the interior S–O band. The $(H_2O)_4$ cluster has a different H bonding pattern to the rest of the water cluster than has W13-1, thus the band shifting.

A discussion on the computed spectra of W13-5 and W13-7 may be found as Section S62 in the ESI.†

Comparison of experimental and computed spectra makes it clear that the shell-closing 12+1 structure W13-AN described in the literature does not fit. A clear indication is provided by the sulfate antisymmetric stretch bands. While the H_2O molecule in the second shell breaks the quasi-C_3 symmetry of the $SO_4^{2-}(H_2O)_{12}$ core, the degeneracy lift of the 3 frequencies is clearly insufficient to account for the experimental width of *ca.* 200 cm^{-1}, contrary to those of the structures described above. In addition, the band at 902 cm^{-1} is in significantly worse agreement with the 970 cm^{-1} experimental band than those of most structures described above, which lie either in the 940–960 or 990 cm^{-1} range. Thus the inescapable conclusion is that the first hydration shell is not closed at n = 13. Interestingly, the wide water libration massif is somewhat different for W13-AN than for the others displayed in Fig. 4, better matching the experimental features on the red side.

4. Discussion

A. Comparison with previous computations

The present results indicate that nearly all structures published previously for $SO_4^{2-}(H_2O)_{12}$ are of high energy. The single exception is from the work of Galli *et al.*[27] with which the present results are qualitatively consistent. There are however considerable quantitative differences, as the more extensive structural search performed herein has allowed identification of a number of new low energy structures. The present results, obtained at the DLPNO-CCSD(T)/aug-cc-pVTZ level, are also expected to be more reliable than the PBE0 results obtained previously. As a consequence, the interpretation[27] of IR spectra in terms of a mixture of surface and interior structures being formed experimentally is unlikely to hold, both in terms of energy and of IR spectra. Kinetic trapping of high energy structures such as W12-AN and W13-AN during cryogenic cooling is not expected to occur for non-covalent complexes which can interconvert through small energy barriers. Our results do support a mixture of several structures of very similar stability, especially for n = 13, however at very low temperature all have the sulfate near the cluster surface.

It remains that the agreement between the present computations and experimental spectra is unsatisfactory in the 600–900 cm^{-1} region. BOMD computations by Galli *et al.*[27] have shown significant improvement over static calculations in this frequency range. It would be very interesting to run BOMD calculations with the lowest energy structures found herein as starting point. In addition, our picture for n = 13, in which the 13th water molecule can move around a compact $SO_4^{2-}(H_2O)_{12}$ core, may be associated with large configurational entropy, which our current approach does not treat. BOMD calculations on such structures may be revealing in this respect.

B. Comparison of IR spectra of $SO_4^{2-}(H_2O)_{12}$ and $SO_4^{2-}(H_2O)_{13}$

The most stable structure for n = 13 has lowered symmetry compared to that for n = 12 because of the additional water molecule. This leads to a larger degeneracy breaking of the sulfate antisymmetric stretching frequencies at 1130–1150 cm^{-1}, accounting for the larger experimental feature for n = 13, which extends toward 1200 cm^{-1}. Coupling of the sulfate inner S–O stretch with water librations, dominated by those waters interacting with the inner S–O bond, leads to two bands of very similar positions for n = 12 and 13. The sulfate-dominated motion has frequencies of 937 and 946 cm^{-1}, respectively, while the water-dominated motion has frequencies of 1034 and 1037 cm^{-1}, respectively. As these motions are remote from the outer water molecule, their similarity is expected. The computed water libration bands for both n = 12 and 13 do not reproduce the experimental features very well, since the latter extend down to 600 cm^{-1} while calculated intensities are rather small below 700 cm^{-1}. This may be due to the static, harmonic approximation used. They do reproduce, however, the overall blue shift of the blue part of the massif for n = 13 as compared to n = 12, with significantly more numerous bands in the 800–950 cm^{-1} area. This extends as far as a band at 992 cm^{-1}, corresponding to coupled librations in one of the water tetramers, to which the outer water is bound. Since this band appears in a completely silent portion of the n = 12 spectrum, it is one of the two possible assignments for the experimental band at 970 cm^{-1}. In such a scenario, the experimental differences observed in the spectra of n = 12 and 13 do arise from a 13th water molecule lying in the second solvation shell, even though it is unrelated to closing the first. In addition the new band at 970 cm^{-1} is not related to this outer molecule's motion. It is the perturbation of several of the inner water libration modes by this additional molecule which leads to the most visible spectral changes, let aside the degeneracy lift of the sulfate stretches discussed above. The outer water molecule donates two hydrogen bonds, however it receives none. This weaker participation to the hydrogen bond network makes its libration less constrained thus the bands for which its contribution is major appear much farther to the red, at around 700 cm^{-1}.

The computed IR spectra also challenge the view that band assignments can be safely made on the basis of those established for the bulk solution spectrum in the 900–1200 cm^{-1} region. It should be noted that the series of experimental spectra,[23] encompassing n = 4–14, 18 and 24 does show progressive overlap between the water libration and sulfate antisymmetric stretch features from n = 10 to 14, while this no longer exists for n = 18 and 24. There appears to exist a region of intermediate size in which the first and second hydration shells are perturbed enough, compared to the bulk, that some parts of their spectra are not directly comparable.

C. Closure of the first hydration shell

The appearance of a band at 970 cm^{-1} at n = 13 appears not to be related to hydration shell closure at n = 12. The single low-energy saturated isomer found for n = 12 (W12-2) does not appear to generate a low-energy isomer for n = 13 by simple addition of H_2O. This is likely due to the smaller binding energy at any site that has to be remote from the ion, compared to W12-1 for which direct access to the charge is possible.

The computed energetics and spectra show that shell closure is still not effected at $n = 13$. In addition, the experimental spectra of $n = 13$ and 14 are strongly similar,[23] including the 970 cm^{-1} band which is common to both. Finally, the shapes of the lowest energy structures for $n = 13$ shown in Fig. 3 suggest that at least one more strongly bound water molecule could easily be accommodated in the second shell. All of these points suggest that closure of the first hydration shell might occur even beyond $n = 14$. At least the experimental IRPD spectra do not provide any indication of shell closure at $n = 14$.

5. Conclusions

Extensive exploration of the potential energy surfaces of $SO_4^{2-}(H_2O)_{12}$ and $SO_4^{2-}(H_2O)_{13}$ and computation of the structures, energetics and IR spectra have been carried out near the current computational accuracy limit. The results provide a new picture of these clusters, as most of the low energy structures identified herein have not been described previously. While the difference in spectra between $n = 12$ and $n = 13$ does provide a structural fingerprint, the latter turns out not to correspond to a qualitative transition in the cluster structure. In particular, it appears not to be related to hydration shell closure at $n = 12$. The computed energetics and spectra show that this closure is still not effected at $n = 13$. In addition, the experimental IRPD spectra of $n = 12$–14 do not provide any indication in favor (nor against) shell closure at $n = 14$.

Comparison of experimental and computed IR spectra also demonstrates that the IR ''fingerprint'' region does not provide a clear identification of a single or a few structures being populated, even at very low temperature. There exists a number of structures, computed to lie in a few kJ mol^{-1} window, whose spectra are compatible with the experimental spectrum. It would be particularly interesting to investigate the O–H stretching portion of IRPD spectra in the 3200–3800 cm^{-1} range to see if more discriminating features can be obtained there.

Finally, it is apparent from the results given in Tables 1 and 2 that even for the small-sized clusters discussed herein, the few most stable isomers may not be the most appropriate tool for structural characterization. Their energies are so similar that except at the very lowest temperatures, a collection of structure families may be required to describe these objects. This will become even truer for larger clusters. To this end, resorting to molecular dynamics (MD) appears to be the method of choice. The results of the present structural search indicate that AMOEBA is a good candidate for running classical MD simulations on hydrated sulfate clusters. IR spectra may then be computed directly from the simulations, as described recently.[37] Such studies are currently underway.

Acknowledgements

We gratefully thank Prof K. R. Asmis for sharing his experimental data of ref. 23, as reproduced in Fig. 2 and 4 of this paper. This work was granted access to the HPC resources of [CCRT/CINES/IDRIS] under the allocation c2015077128 made by GENCI (Grand Equipement National de Calcul Intensif).

References

1 B. J. Finlayson-Pitts and J. N. Pitts Jr., *Chemistry of the upper and lower atmosphere – theory, experiments and applications*, Academic Press, San Diego, 2000.
2 S. Twomey, *Atmospheric aerosols*, Elsevier, New York, 1977.
3 A. Laaksonen, M. Kulmala, T. Berndt, F. Stratmann, S. Mikkonen, A. Ruuskanen, K. E. J. Lehtinen, M. Dal Maso, P. Aalto and T. Petäjä, *et al.*, *Atmos. Chem. Phys.*, 2008, **8**, 7255.
4 V. Ramanathan, P. J. Crutzen, J. T. Kiehl and D. Rosenfeld, *Science*, 2001, **294**, 2119–2124.
5 D. Markovich, *Physiol. Rev.*, 2001, **81**, 1499–1533.
6 J. T. O'Brien, J. S. Prell, M. F. Bush and E. R. Williams, *J. Am. Chem. Soc.*, 2010, **132**, 8248–8249.
7 J. T. O'Brien and E. R. Williams, *J. Am. Chem. Soc.*, 2012, **134**, 10228–10236.
8 A. I. Boldyrev and J. Simons, *J. Phys. Chem.*, 1994, **88**, 2298–2300.
9 A. Whitehead, R. Barrios and J. Simons, *J. Chem. Phys.*, 2002, **116**, 2848–2851.
10 X. B. Wang, J. B. Nicholas and L. S. Wang, *J. Chem. Phys.*, 2000, **113**, 10837–10840.
11 A. T. Blades and P. Kebarle, *J. Am. Chem. Soc.*, 1994, **116**, 10761–10766.
12 C. C. Pye and W. W. Rudolph, *J. Phys. Chem. A*, 2001, **105**, 905–912.
13 C. G. Zhan, F. Zheng and D. A. Dixon, *J. Chem. Phys.*, 2003, **119**, 781–793.
14 B. Gao and Z. F. Liu, *J. Chem. Phys.*, 2004, **121**, 8299–8306.
15 B. Gao and Z. Liu, *J. Chem. Phys.*, 2005, **123**, 224302.
16 Y. Miller, G. M. Chaban, J. Zhou, K. R. Asmis, D. M. Neumark and R. B. Gerber, *J. Chem. Phys.*, 2007, **127**, 094305.
17 M. F. Bush, R. J. Saykally and E. R. Williams, *J. Am. Chem. Soc.*, 2007, **129**, 2220–2221.
18 X. B. Wang, A. P. Sergeeva, J. Yang, X. P. Xing, A. I. Boldyrev and L. S. Wang, *J. Phys. Chem. A*, 2009, **113**, 5567–5576.
19 D. S. Lambrecht, G. N. I. Clark, T. Head-Gordon and M. Head-Gordon, *J. Phys. Chem. A*, 2011, **115**, 11438–11454.
20 D. S. Lambrecht, L. McCaslin, S. S. Xantheas, E. Epifanovsky and M. Head-Gordon, *Mol. Phys.*, 2012, **110**, 2513–2521.
21 N. Mardirossian, D. S. Lambrecht, L. McCaslin, S. S. Xantheas and M. Head-Gordon, *J. Chem. Theory Comput.*, 2013, **9**, 1368–1380.
22 X. B. Wang, X. Yang, J. B. Nicholas and L. S. Wang, *Science*, 2001, **294**, 1322–1325.
23 J. Zhou, G. Santambrogio, M. Brümmer, D. T. Moore, L. Wöste, G. Meijer, D. M. Neumark and K. R. Asmis, *J. Chem. Phys.*, 2006, **125**, 111102.
24 R. L. Wong and E. R. Williams, *J. Phys. Chem. A*, 2003, **107**, 10976–10983.

25 A. T. Blades, J. S. Klassen and P. Kebarle, *J. Am. Chem. Soc.*, 1995, **117**, 10563–10571.
26 A. T. Blades and P. Kebarle, *J. Phys. Chem. A*, 2005, **109**, 8293–8298.
27 Q. Wan, L. Spanu and G. Galli, *J. Phys. Chem. B*, 2012, **116**, 9460–9466.
28 S. Katsyuba and E. Vandyukova, *Chem. Phys. Lett.*, 2003, **377**, 658–662.
29 A. Sharma, G. Ohanessian and C. Clavaguéra, *J. Mol. Model.*, 2014, **20**, 2426–2434.
30 (*a*) C. Riplinger, B. Sandhoefer, A. Hansen and F. Neese, *J. Chem. Phys.*, 2013, **139**, 134101; (*b*) M. Sparta and F. Neese, *Chem. Soc. Rev.*, 2014, **43**, 5032–5041.
31 J. W. Ponder, *Tinker 6 – Software Tools for Molecular Design*, 2010, available at http://dasher.wustl.edu/tinker.
32 M. J. Frisch, *et al.*, *Gaussian09, rev. D.01*, Gaussian, Inc., Wallingford CT, 2013.
33 Turbomole V6.6 2013, a development of University of Karlsruhe and Forschungszentrum Karlsruhe GmbH, 1989–2007, TURBOMOLE GmbH, since 2007, available at http://www.turbomole.com.
34 F. Neese, Orca version 3.0.3., *WIREs Comput. Mol. Sci.*, 2012, **2**, 73–78, available at http://www.thch.uni-bonn.de/tc/orca/.
35 L. C. Smeeton, J. D. Farrell, M. T. Oakley, D. J. Wales and R. L. Johnston, *J. Chem. Theory Comput.*, 2015, **11**, 2377–2384.
36 W. R. Cannon, B. M. Pettitt and J. A. McCammon, *J. Phys. Chem.*, 1994, **98**, 6225–6230.
37 D. Semrouni, A. Sharma, J.-P. Dognon, G. Ohanessian and C. Clavaguéra, *J. Chem. Theory Comput.*, 2014, **10**, 3190–3199.